Damping of Rabi oscillations in intensity-dependent photon echoes from exciton complexes in a CdTe/(Cd,Mg)Te single quantum well

S. V. Poltavtsev,[1,2,*] M. Reichelt,[3] I. A. Akimov,[1,4] G. Karczewski,[5] M. Wiater,[5] T. Wojtowicz,[5,6] D. R. Yakovlev,[1,4] T. Meier,[3] and M. Bayer[1,4]

[1]*Experimentelle Physik 2, Technische Universität Dortmund, D-44221 Dortmund, Germany*
[2]*Spin Optics Laboratory, Saint Petersburg State University, 198504 Saint Petersburg, Russia*
[3]*Department Physik and CeOPP, Universität Paderborn, D-33098 Paderborn, Germany*
[4]*Ioffe Physical-Technical Institute, Russian Academy of Sciences, 194021 Saint Petersburg, Russia*
[5]*Institute of Physics, Polish Academy of Sciences, PL-02668 Warsaw, Poland*
[6]*International Research Centre MagTop, PL-02668 Warsaw, Poland*

(Received 20 June 2017; published 18 August 2017)

We study Rabi oscillations detected in the coherent optical response from various exciton complexes in a 20-nm-thick CdTe/(Cd,Mg)Te quantum well using time-resolved photon echoes. In order to evaluate the role of exciton localization and inhomogeneous broadening we use selective excitation with spectrally narrow ps pulses. We demonstrate that the transient profile of the photon echo from the localized trion (X^-) and the donor-bound exciton (D^0X) transitions strongly depends on the strength of the first pulse. It acquires a non-Gaussian shape and experiences significant advancement for pulse areas larger than π due to non-negligible inhomogeneity-induced dephasing of the oscillators during the optical excitation. Next, we observe that an increase of the area of either the first (excitation) or the second (rephasing) pulse leads to a significant damping of the photon echo signal, which is strongest for the neutral excitons and less pronounced for the donor-bound exciton complex (D^0X). The measurements are analyzed using a theoretical model based on the optical Bloch equations which accounts for the inhomogeneity of optical transitions in order to reproduce the complex shape of the photon echo transients. In addition, the spreading of Rabi frequencies within the ensemble due to the spatial variation of the intensity of the focused Gaussian beams and excitation-induced dephasing are incorporated in our model, which is able to explain the fading and damping of Rabi oscillations. By analyzing the results of the simulation for X^- and D^0X complexes we are able to establish a correlation between the degree of localization and the transition dipole moments determined as $\mu(X^-)$=73 D and $\mu(D^0X)$=58 D.

DOI: 10.1103/PhysRevB.96.075306

I. INTRODUCTION

Coherent control of excitonic states in semiconductor nanostructures under resonant excitation with intense optical pulses attracts a lot of attention in relation to possible applications in quantum information [1]. Such a control exploits coherent rotations of the Bloch vector in the photoexcited two-level system (TLS), which depends on the area of the exciting pulse via Rabi oscillations [2–4]. Since stronger localization of excitons is in favor of longer decoherence times, most of the studies of coherent control have concentrated on quantum dots (QDs) [3,5,6]. However, the strong localization in QDs is accompanied by large variations in QD size, shape, and composition, which leads to the large inhomogeneous broadening of the optical transitions in an ensemble of QDs. Therefore, most Rabi oscillation studies were performed on single QDs [7–10].

In semiconductor quantum well (QW) structures the inhomogeneous broadening of the optical transitions is significantly smaller as compared to QD systems, i.e., it is possible to selectively address different exciton complexes, such as free and localized excitons, localized charged excitons (trions, X^-), and donor-bound excitons (D^0X). Therefore, QW structures can be considered as a model system for the investigation of Rabi oscillations and their damping for optical excitations with different degree of localization and inhomogeneity. In spite of this fact, so far only a few studies on Rabi oscillations have been performed in QW structures [11,12]. This is mainly due to the presence of many-body interactions, which can, however, be suppressed by using spectrally narrow optical pulses [13–15]. Another important issue is related to the detection of Rabi oscillations. One of the approaches is based on reading out of the excited-state population [3,4,11], while another exploits direct measurements of the coherent optical response [6,12]. Due to the inhomogeneous broadening of optical transitions in the TLS ensemble, the coherent optical response in a four-wave-mixing (FWM) experiment is represented by photon echoes [16]. In contrast to single pulse excitation, in FWM the amplitude and the transient profile of the detected signal depend sensitively on the optical field amplitude A_i (pulse area Θ_i) of both exciting ($i = 1$) as well as rephasing ($i = 2$) pulses, which, as is demonstrated below, provides valuable information on the relevant physical effects.

In this paper, we study the coherent optical response for intense resonant excitation of various exciton complexes with different degrees of localization and inhomogeneity in a single CdTe/(Cd,Mg)Te QW structure. In low-temperature measurements we observe photon echoes (PEs) from the ensembles of individually addressed states of localized excitons, trions, and donor-bound excitons. By scanning the areas of the incident pulses and measuring the temporal profiles of photon echo for each exciton complex we observe Rabi oscillations in the form of two-dimensional images similar to those observed recently

*sergei.poltavtcev@tu-dortmund.de

in an ensemble of InAs/(In,Ga)As quantum dots [17]. The images vary for the different complexes because they are very sensitive to the degree of inhomogeneous broadening of the optical transition. Additionally, the photon echoes are strongly damped for large pulse areas. In order to explain this damping, we develop a theoretical model, which takes into account the two most important damping mechanisms: (i) excitation-induced dephasing (EID), which results in the accelerated decay of the coherence with increasing excitation intensity, and (ii) a fading of the Rabi oscillations due to the spatial distribution of the optical excitation. Our results demonstrate that the ensemble of D^0X complexes in CdTe QW structures with low donor concentrations ($n_d \leqslant 10^{10}$ cm^{-2}) is a fairly good two-level system for the generation of intense photon echoes with the $\pi/2 - \pi$ pulse area sequence. However, larger excitation densities lead to unavoidable many-body effects and heating of the electron system, which destroy the coherence and diminish the photon echo signals.

The paper is organized as follows. In Sec. II we describe the experimental technique that is used to measure Rabi oscillations and give details of the studied sample. In Sec. III the experimental results of photon echoes and Rabi oscillation measurements are presented. This is followed by the theoretical analysis of experimental results given in Sec. IV together with the discussion. Finally, conclusions are provided in Sec. V.

II. EXPERIMENTAL METHOD AND SAMPLE

In order to investigate photon echoes we used the time-resolved degenerate FWM technique with optical heterodyning. The optical excitation of the sample was performed using picosecond pulses emitted by a tunable Ti:sapphire laser with a repetition rate of 75.75 MHz. The sample was immersed in liquid helium and cooled down to the temperature of 1.8 K. It was excited by a sequence of two laser pulses separated by a variable delay τ_{12} hitting the sample under the incidence angles of 3° and 4° ($\boldsymbol{k}_1$ and $\boldsymbol{k}_2$), respectively, and focused on the sample to a spot with diameter of about 300 μm. The FWM signal was collected in reflection geometry in the $2\boldsymbol{k}_2 - \boldsymbol{k}_1$ direction, as schematically shown in Fig. 1. This signal was mixed with the optical field of a reference pulse delayed with respect to the first pulse by τ_{Ref} at the balanced detector using a nonpolarizing beamsplitter. All laser pulses including both exciting pulses and the reference pulse were linearly

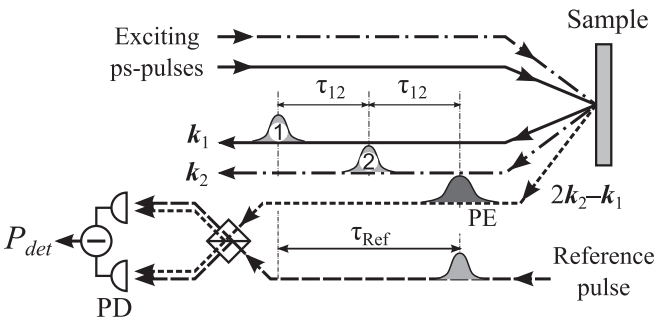

FIG. 1. Scheme of photon echo detection in reflection geometry. PD denotes the photodetector.

copolarized. For heterodyne FWM measurements, the optical frequencies of the first exciting beam and the reference beam were shifted using acousto-optical modulators by −41 and +40 MHz, respectively. The modulus of the cross correlation of the FWM amplitude P_{FWM} with the Gaussian reference pulse field detected at the frequency of 1 MHz is described by

$$P_{\mathrm{det}}(\tau_{\mathrm{Ref}}) \sim \left| \int_{-\infty}^{+\infty} P^*_{\mathrm{FWM}}(\tau_{\mathrm{Ref}} - t') \times \exp\left(-t'^2/2\tau_P^2\right) dt' \right|. \quad (1)$$

Here, $2\sqrt{\ln 2}\tau_P = 2.2$ ps is the laser pulse duration in the intensity scale.

To study the coherent optical dynamics of the localized exciton complexes we chose a structure with a high-quality 20-nm-thick single CdTe QW grown by molecular-beam epitaxy. The structure was grown on (100)-oriented GaAs substrate followed by a 4.5-μm-thick $Cd_{0.76}Mg_{0.24}Te$ buffer and five short-period superlattices separated by 100-nm CdMgTe spacers. This is followed by the QW sandwiched between the 100-nm $Cd_{0.76}Mg_{0.24}Te$ barriers. The structure was not intentionally doped with donors. The resident electron density due to an unavoidable background of impurities is estimated to be $n_d \leqslant 10^{10}$ cm^{-2}. Recent studies performed on this sample have demonstrated the presence of two very closely located optical transitions corresponding to the negatively charged trion (X^-) and the neutral donor-bound exciton (D^0X) at 1.5980 and 1.5972 eV, respectively [18], which are clearly seen in the photoluminescence (PL) spectrum measured at a temperature of 2 K [see Fig. 2(a)]. Additionally, it displays the neutral exciton line (X) located at 1.6005 eV. In order to increase the density of resident electrons, which are required for the excitation of the trion, an additional weak above-barrier illumination from a spectrally broad white light source was used.

III. EXPERIMENTAL RESULTS

Figure 2(b) displays a typical FWM transient measured at $\tau_{12} = 40$ ps, in which a single PE peak at $2\tau_{12} = 80$ ps is seen. To obtain the optical coherence time T_2^0, the delay τ_{12} was varied and the PE amplitude was detected at $\tau_{\mathrm{Ref}} = 2\tau_{12}$ in the regime of weak optical excitation. This procedure was performed for a number of spectral positions, and Fig. 2(c) displays three PE decays measured on the donor-bound exciton at $E(D^0X)$=1.5972 eV, the trion at $E(X^-)$=1.5980 eV, and the localized exciton state at $E(X_L)$=1.5990 eV. These decays are well fitted by the exponential decay function $\sim\exp(-\tau_{12}/2T_2^0)$, which provides the following values of the coherence time: $T_2^0(D^0X)$=96 ps, $T_2^0(X^-)$=75 ps, and $T_2^0(X_L)$=20 ps. Corresponding homogeneous linewidths $\hbar\gamma_0 = \hbar/T_2^0$ are $\hbar\gamma_0(D^0X)$=6.9 μeV, $\hbar\gamma_0(X^-)$=8.8 μeV, and $\hbar\gamma_0(X_L)$=33 μeV. The spectral dependencies of T_2^0 and $\hbar\gamma_0$, shown in Fig. 2(a), are measured in a similar way. From these data one can see that the donor-bound exciton and trion have long coherence times up to 100 ps, while the free excitons located at energies above 1.6005 eV reveal a very short T_2^0 of below 10 ps. The optical transitions in the region of 1.599–1.600 eV have moderate coherence times on the order of 20 ps, which we attribute to localized exciton states. It is worth

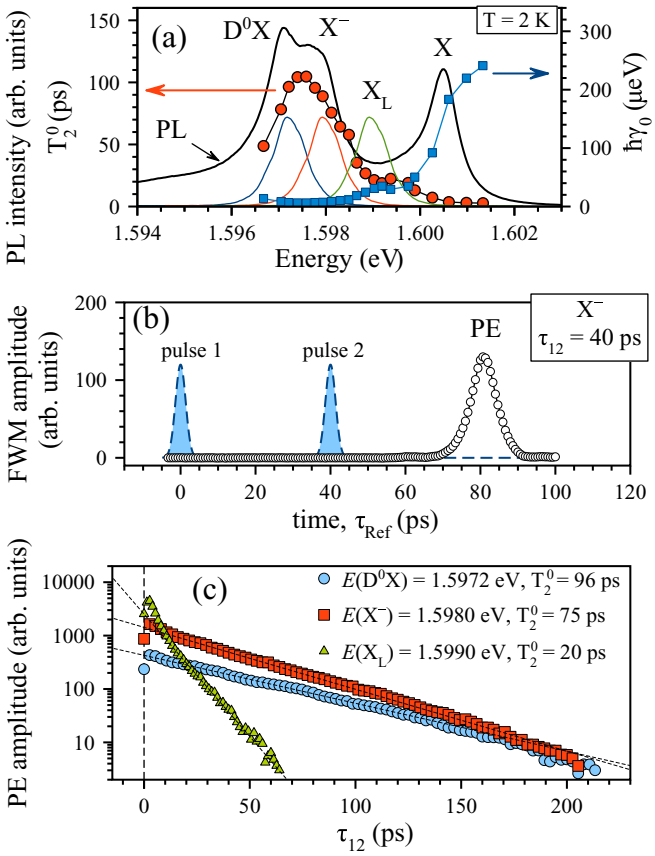

FIG. 2. (a) PL spectrum of the studied sample (black line) with indicated spectral features: donor-bound exciton at $E(D^0X)$=1.5972 eV, trion at $E(X^-)$=1.5980 eV, and neutral exciton at $E(X)$=1.6005 eV. Spectra of laser pulses tuned to D^0X, X^-, and the localized exciton state (X_L) are shown by the blue, red, and green lines, respectively. Red dots are the coherence times T_2^0 and blue dots are the homogeneous linewidths $\hbar\gamma_0$ obtained from scans of the PE decays. (b) Transient of FWM signal measured at the trion at $\tau_{12} = 40$ ps demonstrating a PE located at $\tau_{\mathrm{Ref}} = 2\tau_{12} = 80$ ps (circles). The exciting pulses are schematically shown by the dashed line. (c) Decays of the PE amplitude measured at three indicated energies with extracted coherence times T_2^0.

noting that the low-energy side of the donor-bound exciton below 1.5975 eV shows some shortening of the coherence times down to 50 ps, while the exciton and the trion show an increase of T_2^0 with decreasing excitation energy. The degree of the exciton and the trion localization on the potential and composition fluctuations increases with the energy decrease. Thus, longer T_2^0 times are expected for lower-energy excitons and trions [13]. For D^0X, the transition energy is known to be affected by other factors, in particular, the interaction between neighboring donors [19]. Thus, the spectral dependence of T_2^0 for D^0X can be more complex and is clearly different from that of the localized exciton and trion.

In order to observe Rabi oscillations, PE transients similar to that shown in Fig. 2(b) were recorded as a function of the amplitude of one of the two exciting pulses, A_i ($i = 1,2$), which we define as the square root of the energy per pulse, while that of the other pulse was kept constant. Thus, we vary the exciting pulse areas Θ_i ($i = 1,2$) and keep the pulse duration τ_P fixed. Figure 3 summarizes the experimental results obtained at the three spectral positions indicated above.

The excitation of the localized exciton at $E(X_L)$=1.5990 eV results in a PE positioned at $2\tau_{12} \approx 53$ ps, as shown in Fig. 3(b). Here, the first pulse amplitude A_1 was scanned using a constant $A_2 = 3.5$ pJ$^{1/2}$. The PE amplitude becomes damped at $A_1 \approx 7$ pJ$^{1/2}$ and no oscillatory behavior can be observed. This behavior is to be expected since the nonlinear response of free and weakly localized excitons is very strongly affected by many-body interactions that lead to rapid dephasing and thus prevent the appearance of oscillatory intensity-dependent echo signals [20–22].

The same type of measurement performed on the trion at $E(X^-)$=1.5980 eV and shown on the upper panel of Fig. 3(c) displays a drastically different result. When the first pulse amplitude A_1 is varied at $A_2 = 3.5$ pJ$^{1/2}$, the PE transients reveal a complex two-dimensional picture with the split PE profile similar to that observed recently in (In,Ga)As quantum dots [17]. The first maximum of the Rabi oscillations for $A_1 = 3.6$ pJ$^{1/2}$ is centered at $2\tau_{12} \approx 53$ ps and well described by a single pulse of Gaussian shape, which is expected for a Hahn echo [23]. However, the second maximum at $A_1 = 13$ pJ$^{1/2}$ is significantly advanced. The tail of the third maximum of Rabi oscillations at $A_1 > 20$ pJ$^{1/2}$ appears to be nonshifted. When the amplitude of the second pulse A_2 is varied at $A_1 = 3.5$ pJ$^{1/2}$, the PE maximum has no shift, as can be seen from the upper panel of Fig. 3(d). Here, however, only the first maximum of Rabi oscillations at $A_2 = 7.5$ pJ$^{1/2}$ is pronounced, while the second one around $A_2 = 20$ pJ$^{1/2}$ is very weak. This is better visible in Fig. 3(a), where the cross sections of the two-dimensional plots of Rabi oscillations according to the variations of both pulse amplitudes are plotted.

Figure 3(e) displays the measurement of Rabi oscillations performed on the donor-bound exciton at $E(D^0X)$=1.5972 eV. Here, when A_1 is varied at $A_2 = 3.4$ pJ$^{1/2}$, the PE transients appear somewhat broader in time as compared to those measured on the trion. This means that the optically excited inhomogeneous ensemble of D^0X is narrower than that for the trion. Also, the transition dipole moment of D^0X is smaller than that of X^-, since the Rabi frequency is smaller.

IV. THEORETICAL MODEL AND DISCUSSION

The experimental measurements clearly manifest a rich intensity-dependent coherent behavior of the donor-bound exciton and the trion, which can be analyzed by modeling them as inhomogeneous ensembles of two-level systems interacting with the optical field. This approach is, however, unlikely to be applicable to the localized excitons X, the dynamics of which is more strongly influenced by complex many-body correlations [20–22] that may not be described properly by the modeling used here. In the following we develop an adapted theoretical model that is able to describe the observed intensity dependence of PEs measured on D^0X and X^- and study the mechanisms responsible for the observed damping of the Rabi oscillations.

To simulate the photon echo transients, we numerically solve sets of the optical Bloch equations [23,24], i.e., the coupled equations of motion for the microscopic polarization p and the occupation of the excited state n, considering excitation

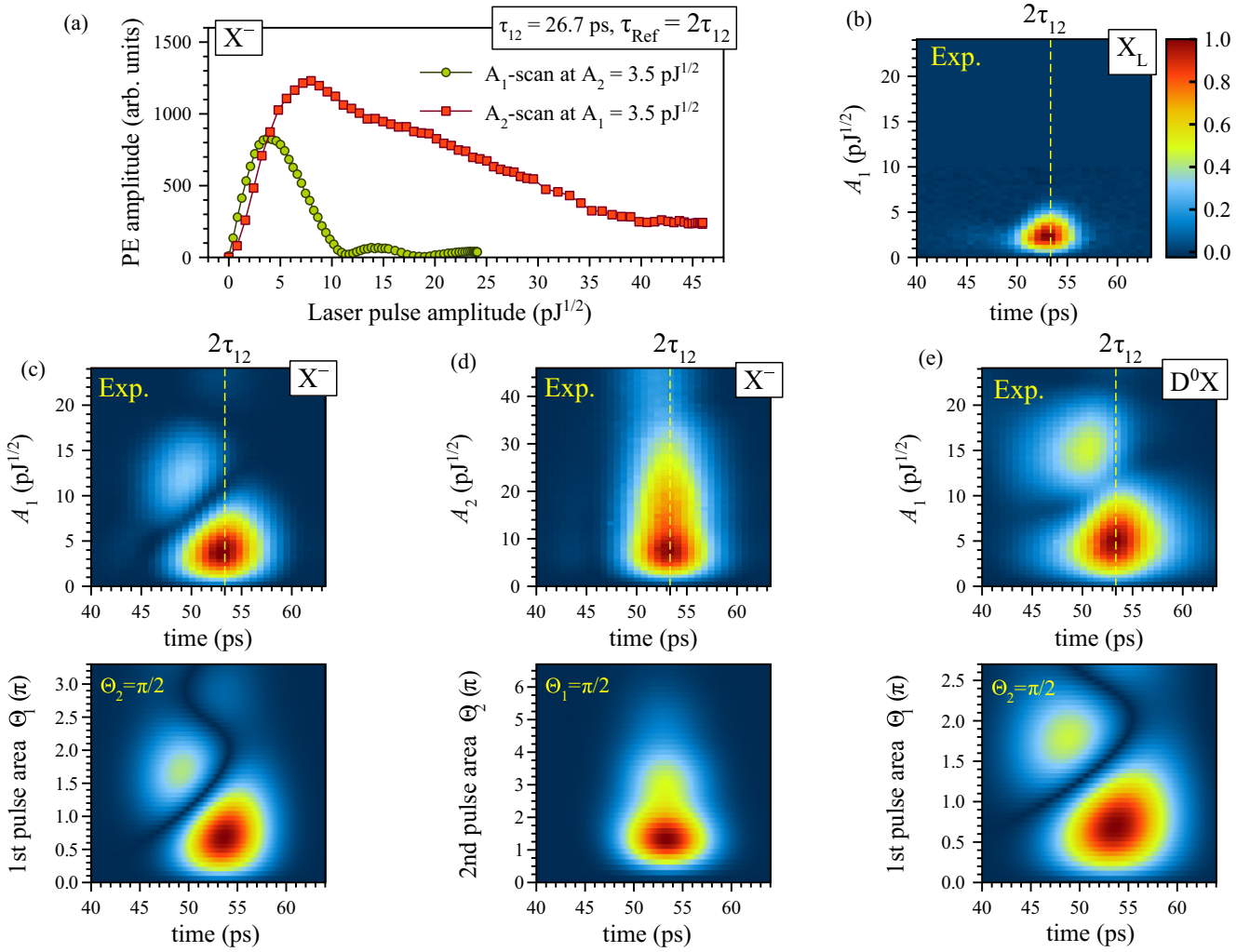

FIG. 3. Rabi oscillations measured on the various localized exciton complexes in the studied CdTe/(Cd,Mg)Te QW. (a) Dependence of PE amplitude measured on the trion ($E = 1.5980$ eV) detected at $\tau_{\mathrm{Ref}} = 2\tau_{12} = 53.3$ ps on both pulse amplitudes. Measurements of PE transients as a function of pulse amplitude: (b) localized exciton at $E(\mathrm{X_L})$=1.5990 eV, A_1 is varied at $A_2 = 3.5$ pJ$^{1/2}$; (c) localized trion at $E(\mathrm{X^-})$=1.5980 eV, A_1 is varied at $A_2 = 3.5$ pJ$^{1/2}$; (d) A_2 is varied at $A_1 = 3.5$ pJ$^{1/2}$; and (e) donor-bound exciton at $E(\mathrm{D^0X})$=1.5972 eV, A_1 is varied at $A_2 = 3.4$ pJ$^{1/2}$. Upper and lower panels of (c)–(e) are the experimental data (upper row) and the numerical simulations (lower row), respectively. The scales in panels (b)–(e) are normalized to unity.

parameters corresponding to the experimental situations. Since an adequate explanation of the experimental results requires the incorporation of a number of effects, which are described in more detail below, the numerically solved system of equations contains two indices f and s:

$$\frac{\partial}{\partial t} p_{f,s}(t) = [-i\,\omega_f - \gamma(t)]\, p_{f,s}(t) + i\frac{\mu}{\hbar}\mathcal{E}_s(t)[1 - 2n_{f,s}(t)], \tag{2}$$

$$\frac{\partial}{\partial t} n_{f,s}(t) = -2\frac{\mu}{\hbar}\,\mathrm{Im}[p_{f,s}(t)^*\mathcal{E}_s(t)]. \tag{3}$$

Here, ω_f is the optical transition frequency of the TLS, μ is the dipole matrix element which is taken to be constant for the ensemble, $\mathcal{E}_s$ is the total electric field including both laser pulses, $\mathcal{E}(t) = \mathcal{E}_1(t) + \mathcal{E}_2(t)$, and $\gamma(t)$ is the excitation and thus time-dependent dephasing rate. Even a qualitative explanation of the experimental findings requires one to incorporate three effects into the theoretical analysis: (i) an inhomogeneous broadening of the resonance, i.e., a Gaussian distribution of the optical frequency within the TLS ensemble which is described by the f; (ii) the spatial profile of the incident laser pulses which is described as a Gaussian leading to the additional index s; and (iii) excitation-induced dephasing, which is caused by the amount of optical excitation and, therefore, leads to the time-dependent dephasing rate $\gamma(t)$.

By solving the system of equations (2) and (3) we compute the total FWM polarization describing photon echoes as

$$P_{\mathrm{FWM}}(t) = \sum_{f,s} \mu\,\alpha_f\,\beta_s\,p_{f,s}(t), \tag{4}$$

where α_f and β_s are weight coefficients described further below. To compare with the experimentally detected signal we convolute Eq. (4) with the Gaussian shaped reference pulse, as described by Eq. (1).

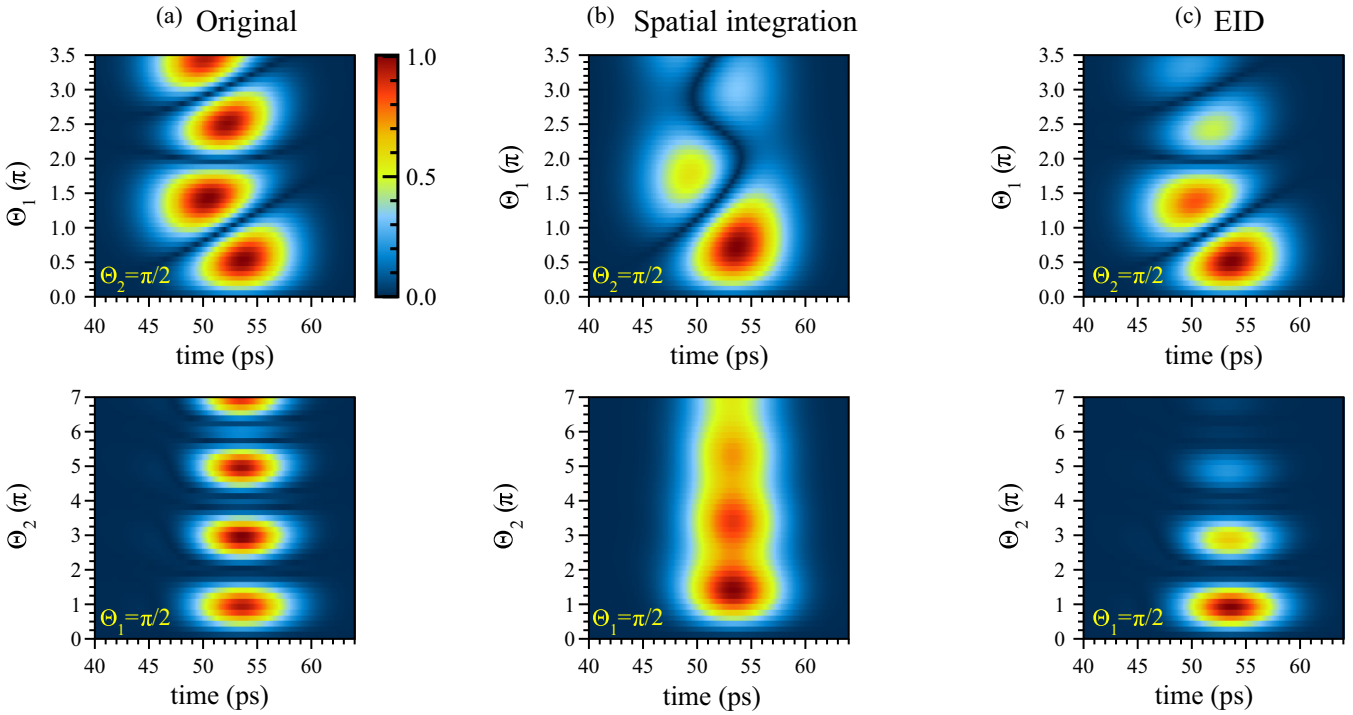

FIG. 4. Various mechanisms responsible for the damping of the simulated Rabi oscillations. (a) Rabi oscillations without damping mechanisms. (b) Only the spatial integration over the excitation beam is activated and $\gamma = 1/T_2^0$. (c) Only EID is activated. Upper panels correspond to the first pulse area scan at $\Theta_2 = \pi/2$; lower panels correspond to the second pulse area scan at $\Theta_1 = \pi/2$. All intensity scales are normalized to unity. The width of the spectral ensemble used in the calculations is $2\sqrt{2\ln 2}\sigma = 1.0$ meV and the pulse delay is $\tau_{12} = 26.7$ ps.

When setting up and solving Eqs. (2) and (3), we take a number of experimental requirements into account.

(i) In order to obtain a photon echo, an inhomogeneous distribution of the optical transition energies is necessary. We define the spectral density of oscillators by a Gaussian distribution $\alpha_f \propto \exp[-(\omega_f - \omega_0)^2/2\sigma^2]$ centered at ω_0, which is coincident with the optical field frequency. Here, we adjust the width σ, such that the temporal profile of the echo calculated at both exciting pulse areas $\Theta_i = \int \frac{\mu}{\hbar}\mathcal{E}_i(t)dt = \pi/2$, $(i = 1,2)$ [23], and the temporal profile of the PE measured at $A_1 \approx A_2 \approx 3.5$ pJ$^{1/2}$ have equal temporal widths.

(ii) We also take into account the spread of Rabi frequencies within the ensemble. A statistical distribution of the dipole moments in the ensemble can result in a variation of the pulse area. However, in contrast to strongly inhomogeneous QD ensembles, this effect is unlikely to take place in a QW structure [25,26]. Here, we, however, have to consider the spatial variation of the pulse within the excitation spot which is modeled by a Gaussian profile $\mathcal{E}_s \sim \exp(-r^2/2\sigma_R^2)$ in real space (r is the distance from the laser spot center), with σ_R characterizing the size of the focused laser beam. This spatial excitation profile defines also a weight $\beta_s \sim r$, which corresponds to the amount of oscillators, located in the sample area with the radius r and excited by the field amplitude $\mathcal{E}_s$. In other words, due to the nonlinear characteristics of the Bloch equations (2) and (3), various Rabi frequencies are superimposed and enter the total signal with according weight β_s. This spatial integration has a profound effect on the Θ_1 and Θ_2 dependencies and leads to an additional decrease of the Rabi oscillation amplitude for the higher pulse areas. This is visualized in Figs. 4(a) and 4(b), where numerically simulated Rabi oscillations are shown for the cases when all dephasing mechanisms are deactivated and only the spatial integration is considered, respectively. Additional to the damping, the effective frequency of the Rabi oscillations is also affected. It should be noted that the result of the calculations does not depend on the value of the beam size σ_R, when the spatial integration is performed for a large enough area [$\max(r) \gtrsim 3\sigma_R$].

(iii) The dephasing rate $\gamma(t) = \gamma[\mathcal{E}(t)]$, which depends on the state of the optical excitation of the system and thus on the exciting electric fields, is a crucial factor in modeling the different experimental situations. It is known that Rabi oscillations can be damped depending on the excitation strengths of the driving fields and quite a few different mechanisms have been identified. The damping might be due to phonons, population leakage into the delocalized states, Auger capture, or the transfer of the excitation to other states [12,27–29]. For the trion and donor-bound exciton, heating of the electronic ensemble in the ground state is also one of the relevant mechanisms [30]. Nevertheless, it has been shown that the specific mechanism is less important than the non-Markovian behavior of a reservoir [31,32]. Here, we assume that for our conditions the intensity dependence of the dephasing rate is governed by excitation-induced dephasing [20,21]. In our simulations we describe this dependence by

$$\gamma(t) = \frac{1}{T_2^0} + a\int_{-\infty}^{t} dt'\mathcal{E}^2(t'). \tag{5}$$

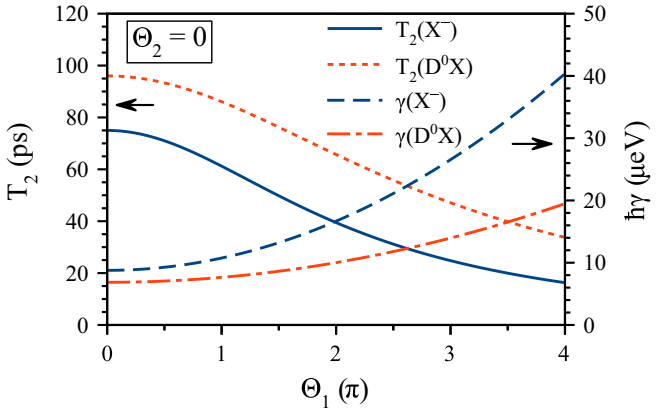

FIG. 5. Calculated excitation-induced dephasing as a function of the first pulse area Θ_1 at $\Theta_2 = 0$: solid and dotted lines are the dephasing times $T_2 = 1/\gamma$ of X^- and D^0X, respectively; dashed and dash-dotted lines are the dephasing rates γ of X^- and D^0X, respectively.

The main idea is that the laser field off-resonantly excites populations that via scattering effects lead to a damping of the polarization. The effect of EID can be seen in Fig. 4(c), where Rabi oscillations are simulated with activated EID without integrating over the spatial coordinate.

By adjusting the model parameters for the effects (i)–(iii), using T_2^0 obtained from the PE decay measurements with weak pulses as well as the proper laser pulse characteristics, one can model and understand the measured echo signals shown in Figs. 3(c)–3(e). Results of the Rabi oscillation simulations are shown in this figure in the lower panels under the according experimental plots. In these simulations, the adjusted spectral widths of the X^- and D^0X ensembles are $2\sqrt{2\ln 2}\sigma = 1.0 \pm 0.1$ and 0.5 ± 0.1 meV, respectively. This ratio of linewidths seems reasonable, since the potential for the donor-bound exciton is less affected by the fluctuations of composition and QW width. The adjusted EID parameter a is different in the two simulations, so that $a(X^-)/a(D^0X)$=2.5, giving significantly different EID for the two considered exciton complexes. This can be seen from Fig. 5, where the calculated dephasing rate γ and the dephasing time $T_2 = 1/\gamma$ are plotted as functions of the first pulse area Θ_1 at $\Theta_2 = 0$. As a result, the Rabi oscillations for the case of donor-bound excitons are more robust. This qualitative conclusion correlates with the assumption that D^0X is more strongly localized than the trion and, hence, many-body interactions leading to EID are weaker for this transition.

Finally, from the Rabi oscillation simulations we can obtain the transition dipole moments for both resonances. In order to calculate them we use the expression for the Rabi frequency, $\Omega_R = \mu\mathcal{E}/\hbar$, and take into account the laser spot size, the pulse duration, and the scale of the Rabi oscillations in units of the pulse amplitude known from the experimental data. As a result, we evaluate $\mu(X^-) \approx 73$ D and $\mu(D^0X) \approx 58$ D. This gives a ratio of $\mu(X^-)/\mu(D^0X) = 1.26$ which can also be deduced from the period of the Rabi oscillations in Figs. 3(c) and 3(e). We can compare this value with another estimation based on first-principles calculations, from which we know that $\mu^2 \sim \tau_0$, where τ_0 is the radiative lifetime of the optical excitation [33]. Values of the optical lifetime T_1 for X^- and D^0X were measured earlier in the same sample at low temperature: $T_1(D^0X)$=66 ps and $T_1(X^-)$=55 ps [18]. Comparing these values with $T_2^0(D^0X)$=96 ps and $T_2^0(X^-)$=75 ps measured here we have the ratio $2T_1 \approx T_2^0$ roughly fulfilled for both transitions for weak optical excitation. This means that the energy decay of both the trion and the donor-bound exciton is mainly radiative, i.e., $\tau_0 \approx T_1$. Thus, we can estimate $\mu(X^-)/\mu(D^0X) \approx \sqrt{T_1(D^0X)/T_1(X^-)} = 1.10$, which is in qualitative agreement with the previous estimation. We can, therefore, conclude that the transition dipole moment of the trion and the donor-bound exciton correlates with the degree of localization of these particles.

V. CONCLUSIONS

We have measured and analyzed optical Rabi oscillations by means of photon echoes from the trion and donor-bound excitons in a CdTe/(Cd,Mg)Te QW structure. The photon echoes detected from the localized exciton states exhibit rapid quenching of the Rabi oscillations which most likely originates from excitation-induced dephasing. Our experimental findings together with the proposed model provide a spectroscopic method by which the coherent evolution of various optical excitations can be studied in detail. By comparing the results of numerical simulations for the D^0X and the X^- complexes we establish a correlation between the degree of localization and the transition dipole moment of the exciton complexes: the stronger localized donor-bound exciton has a smaller μ than the trion (58 and 73 D, correspondingly). It follows that the influence of EID on the coherent response of D^0X is significantly weaker as compared to the localized trion ($\hbar\gamma = 9$ and 14 μeV, respectively, at $\Theta_1 = 3\pi/2$, $\Theta_2 = \pi/2$). The inhomogeneous broadening extracted from the simulations amounts to 0.5 and 1.0 meV for D^0X and X^-, respectively. The experiment and the simulations demonstrate that the Rabi oscillations are strongly smoothed due to the spatially inhomogeneous optical excitation spots. This averaging can be significantly reduced or overcome by using a spatial mask to define a more homogeneously excited sample area, which we consider as a prospect for future studies.

ACKNOWLEDGMENTS

We acknowledge financial support of the Deutsche Forschungsgemeinschaft through the Collaborative Research Centre TRR 142 (Project No. A02) and the International Collaborative Research Centre 160, the latter of which is also supported by the Russian Foundation of Basic Research (Project No. N 15-52-12016 NNIO_a). M.B. acknowledges partial financial support from the Russian Ministry of Science and Education (Contract No. 14.Z50.31.0021). The research in Poland was partially supported by the National Science Centre (Poland) through Grants No. DEC-2012/06/A/ST3/00247 and No. DEC-2014/14/M/ST3/00484, as well as by the Foundation for Polish Science through the International Research Agenda Program cofinanced by the European Union within Smart Growth Operational Program.

[1] M. Fox, *Quantum Optics: An Introduction* (Oxford University Press, New York, 2006).

[2] I. I. Rabi, Space quantization in a gyrating magnetic field, Phys. Rev. **51**, 652 (1937).

[3] T. H. Stievater, X. Li, D. G. Steel, D. Gammon, D. S. Katzer, D. Park, C. Piermarocchi, and L. J. Sham, Rabi Oscillations of Excitons in Single Quantum Dots, Phys. Rev. Lett. **87**, 133603 (2001).

[4] A. Zrenner, S. Beham, E. Stufler, F. Findeis, M. Bichler, and G. Abstreiter, Coherent properties of a two-level system based on a quantum-dot photodiode, Nature (London) **418**, 612 (2002).

[5] Q. Q. Wang, A. Muller, P. Bianucci, E. Rossi, Q. K. Xue, T. Takagahara, C. Piermarocchi, A. H. MacDonald, and C. K. Shih, Decoherence processes during optical manipulation of excitonic qubits in semiconductor quantum dots, Phys. Rev. B **72**, 035306 (2005).

[6] T. Suzuki, R. Singh, M. Bayer, A. Ludwig, A. D. Wieck, and S. T. Cundiff, Coherent Control of the Exciton-Biexciton System in an InAs Self-Assembled Quantum Dot Ensemble, Phys. Rev. Lett. **117**, 157402 (2016).

[7] S. Stufler, P. Ester, A. Zrenner, and M. Bichler, Quantum optical properties of a single $In_xGa_{1-x}As$-GaAs quantum dot two-level system, Phys. Rev. B **72**, 121301(R) (2005).

[8] A. J. Ramsay, R. S. Kolodka, F. Bello, P. W. Fry, W. K. Ng, A. Tahraoui, H. Y. Liu, M. Hopkinson, D. M. Whittaker, A. M. Fox, and M. S. Skolnick, Coherent response of a quantum dot exciton driven by a rectangular spectrum optical pulse, Phys. Rev. B **75**, 113302 (2007).

[9] A. J. Ramsay, A review of the coherent optical control of the exciton and spin states of semiconductor quantum dots, Semicon. Sci. Tech. **25**, 103001 (2010).

[10] L. Monniello, C. Tonin, R. Hostein, A. Lemaitre, A. Martinez, V. Voliotis, and R. Grousson, Excitation-Induced Dephasing in a Resonantly Driven InAs/GaAs Quantum Dot, Phys. Rev. Lett. **111**, 026403 (2013).

[11] A. Schülzgen, R. Binder, M. E. Donovan, M. Lindberg, K. Wundke, H. M. Gibbs, G. Khitrova, and N. Peyghambarian, Direct Observation of Excitonic Rabi Oscillations in Semiconductors, Phys. Rev. Lett. **82**, 2346 (1999).

[12] B. Patton, U. Woggon, and W. Langbein, Coherent Control and Polarization Readout of Individual Excitonic States, Phys. Rev. Lett. **95**, 266401 (2005).

[13] G. Noll, U. Siegner, S. G. Shevel, and E. O. Göbel, Picosecond Stimulated Photon Echo Due to Intrinsic Excitations in Semiconductor Mixed Crystals, Phys. Rev. Lett. **64**, 792 (1990).

[14] L. Langer, S. V. Poltavtsev, I. A. Yugova, D. R. Yakovlev, G. Karczewski, T. Wojtowicz, J. Kossut, I. A. Akimov, and M. Bayer, Magnetic-Field Control of Photon Echo from the Electron-Trion System in a CdTe Quantum Well: Shuffling Coherence Between Optically Accessible and Inaccessible States, Phys. Rev. Lett. **109**, 157403 (2012).

[15] L. Langer, S. V. Poltavtsev, I. A. Yugova, M. Salewski, D. R. Yakovlev, G. Karczewski, T. Wojtowicz, I. A. Akimov, and M. Bayer, Access to long-term optical memories using photon echoes retrieved from semiconductor spins, Nat. Photonics **8**, 851 (2014).

[16] P. R. Berman and V. S. Malinovsky, *Principles of Laser Spectroscopy and Quantum Optics* (Princeton University, Princeton, NJ, 2011).

[17] S. V. Poltavtsev, M. Salewski, Y. V. Kapitonov, I. A. Yugova, I. A. Akimov, C. Schneider, M. Kamp, S. Höfling, D. R. Yakovlev, A. V. Kavokin, and M. Bayer, Photon echo transients from an inhomogeneous ensemble of semiconductor quantum dots, Phys. Rev. B **93**, 121304(R) (2016).

[18] M. Salewski, S. V. Poltavtsev, I. A. Yugova, G. Karczewski, M. Wiater, T. Wojtowicz, D. R. Yakovlev, I. A. Akimov, T. Meier, and M. Bayer, High-Resolution Two-Dimensional Optical Spectroscopy of Electron Spins, Phys. Rev. X **7**, 031030 (2017).

[19] B. Shklovskii and A. Efros, *Electronic Properties of Doped Semiconductors* (Springer, Berlin, 1984).

[20] H. Wang, K. Ferrio, D. G. Steel, Y. Z. Hu, R. Binder, and S. W. Koch, Transient Nonlinear Optical Response from Excitation Induced Dephasing in GaAs, Phys. Rev. Lett. **71**, 1261 (1993).

[21] F. Jahnke, M. Kira, S. W. Koch, G. Khitrova, E. K. Lindmark, T. R. Nelson, Jr., D. V. Wick, J. D. Berger, O. Lyngnes, H. M. Gibbs, and K. Tai, Excitonic Nonlinearities of Semiconductor Microcavities in the Nonperturbative Regime, Phys. Rev. Lett. **77**, 5257 (1996).

[22] H. Haug and S. W. Koch, *Quantum Theory of the Optical and Electronic Properties of Semiconductors*, 5th ed. (World Scientific, Singapore, 2009).

[23] N. Allen and J. H. Eberly, *Optical Resonance and Two-Level Atoms* (Wiley, New York, 1975), Chap. 9.

[24] T. Meier, P. Thomas, and S. W. Koch, *Coherent Semiconductor Optics: From Basic Concepts to Nanostructure Applications* (Springer, New York, 2007).

[25] P. Borri, W. Langbein, S. Schneider, U. Woggon, R. L. Sellin, D. Ouyang, and D. Bimberg, Rabi oscillations in the excitonic ground-state transition of InGaAs quantum dots, Phys. Rev. B **66**, 081306(R) (2002).

[26] M. Salewski, S. V. Poltavtsev, Y. V. Kapitonov, J. Vondran, D. R. Yakovlev, C. Schneider, M. Kamp, S. Höfling, R. Oulton, I. A. Akimov, A. V. Kavokin, and M. Bayer, Photon echoes from (In, Ga)As quantum dots embedded in a Tamm-plasmon microcavity, Phys. Rev. B **95**, 035312 (2017).

[27] P. T. Greenland, S. A. Lynch, A. F. G. van der Meer, B. N. Murdin, C. R. Pidgeon, B. Redlich, N. Q. Vinh, and G. Aeppli, Coherent control of Rydberg states in silicon, Nature (London) **465**, 1057 (2010).

[28] A. Krügel, V. M. Axt, T. Kuhn, P. Machnikowski, and A. Vagov, The role of acoustic phonons for Rabi oscillations in semiconductor quantum dots, Appl. Phys. B **81**, 897 (2005).

[29] H. J. Zhou, S. D. Liu, M. T. Cheng, Q. Q. Wang, Y. Y. Li, and Q. K. Xue, Rabi oscillation damped by exciton leakage and Auger capture in quantum dots, Opt. Lett. **30**, 3213 (2005).

[30] E. A. Zhukov, D. R. Yakovlev, M. M. Glazov, L. Fokina, G. Karczewski, T. Wojtowicz, J. Kossut, and M. Bayer, Optical control of electron spin coherence in CdTe/(Cd, Mg)Te quantum wells, Phys. Rev. B **81**, 235320 (2010).

[31] D. Mogilevtsev, A. Nisovtsev, S. Kilin, S. Cavalcanti, H. Brandi, and L. Oliveira, Non-Markovian damping of Rabi oscillations in semiconductor quantum dots, J. Phys.: Condens. Matter **21**, 055801 (2009).

[32] D. Mogilevtsev, A. P. Nisovtsev, S. Kilin, S. B. Cavalcanti, H. S. Brandi, and L. E. Oliveira, Rabi oscillation damping of two-level states in quantum dots, Physica E **40**, 1487 (2008).

[33] E. L. Ivchenko, *Optical Spectroscopy of Semiconductor Nanostructures* (Alpha Science, Harrow, 2005).